Hertzsprung-Russell Diagrams of Two Messier Clusters

June 2023

1 Introduction

Hertzsprung-Russell diagrams provide insight into the relations between a star's color index, temperature, and luminosity. Both Messier 44 and Messier 13 were selected to create H-R diagrams because of their close relative proximity to Earth and seasonal visibility. Imaging was completed using Las Cumbres Observatory's (LCO) SBIG 6303 0.4m class telescopes from various observation sites. Image processing was completed in part with AstroArt, and further evaluation of data was completed using the AstroPy Python package. The two main components of this project are astrophotography and analysis via H-R diagrams. This project demonstrates the differences between open and globular clusters in terms of age and density. Analysis of images captured provides information on signal-to-noise ratios, sources of error, and key observations.

2 Historical Background

2.1 Star Clusters

In general, open clusters contain young stars that allow for "main sequence mapping". This method involves calculating luminosity from the common age and varying masses of the stars in the cluster. In contrast, globular clusters are substantially older and much more massive. Thus, globular clusters have a higher proportion of red giants and low-mass main-sequence stars.

2.1.1 Messier 44 (NGC 2632)

Messier 44, known as Praesepe or the Beehive Cluster, has been observed since ancient times. It is roughly 577 light-years from Earth and spans 15 light-years, making it one of the closest star clusters to Earth. It also has a mass of about 500-600 Solar mass. The Beehive Cluster is an open cluster that it contains about 1,000 stars; they are mostly young stars and have approximate age of 600 million years. Of these stars, 68% are M-class red dwarfs, 2% are class A, and the remaining 30% belong to spectral classes F, G, and K, with

a few minor exclusions in the form of dying white dwarfs [5]. The average apparent magnitude of M44 is 3.7, however, there are brighter stars with an apparent magnitude much brighter than this. In the context of this project, the apparent magnitude was calculated based on the near infrared-filtered images taken, as described in section 4.

Figure 1: This image of M44 is an "Atlas Image obtained as part of the Two Micron All Sky Survey (2MASS), a joint project of the University of Massachusetts and the Infrared Processing and Analysis Center/California Institute of Technology, funded by the National Aeronautics and Space Administration and the National Science Foundation"[5].

2.1.2   Messier 13 (NGC 6205)

Messier 13, otherwise known as the Hercules Globular Cluster, was first discovered in 1714 by Edmond Halley and later cataloged by Charles Messier into the Messier catalog. It lies 22.7-kilo light-years away from Earth and is 145 light-years in diameter, with a mass of 6×10^5 solar masses. It is potentially visible to the naked eye with an apparent magnitude of +5.8. M13 is a class V globular cluster, with most of its stars densely packed in the central region [3]. It is estimated to be 11.65 billion years old with about 300,000 stars. The brightest star in M13 is a red giant with a visual magnitude of 11.95. Other stars in the cluster are relatively old and have been determined to have been formed before the stars in our galaxy created metals based on their low iron percentage. Messier 13 also contains roughly 15 blue, young stars.

Figure 2: Image captured by Adam Block and Sid Leach at Mount Lemmon SkyCenter at the University of Arizona [3].

2.2 Hertzsprung-Russell Diagrams

Hertzsprung-Russell diagrams have been used by astronomers since the early twentieth century. In 1911 Ejnar Hertzsprung made a chart plotting a star's magnitudes and colors (which relates to effective temperature); later in 1913, Henry Norris Russell used the same idea to group stars based on their luminosity and spectral class [4]. The resulting plots displayed that the relationship between the temperature of stars was not random, but could be categorized into specific groupings.

3 Theory

In Hertzsprung-Russell diagrams that plot surface temperature versus luminosity, there are often three main groups of stars, the main sequence, giants, and super-giants. Stars "spend about 90% of their life in the main-sequence stage," [4] that main sequence turnoff signifies where stars begin the end of their life cycle. In the bottom-left of the plot, white dwarf stars and red giants/super-giants can be found in the top-right. Stars' class, color, magnitude, and temperature can be used in these plots because stars are considered black-body sources. Luminosity can be calculated based on the relation:

$$L = 4\pi R^2 \sigma T^4 \tag{1}$$

[2] This describes the ability of luminosity to vary so widely across similar-class stars, in relation to their size. The most luminous stars are super-giants, and the dim stars are part of the main sequence, otherwise
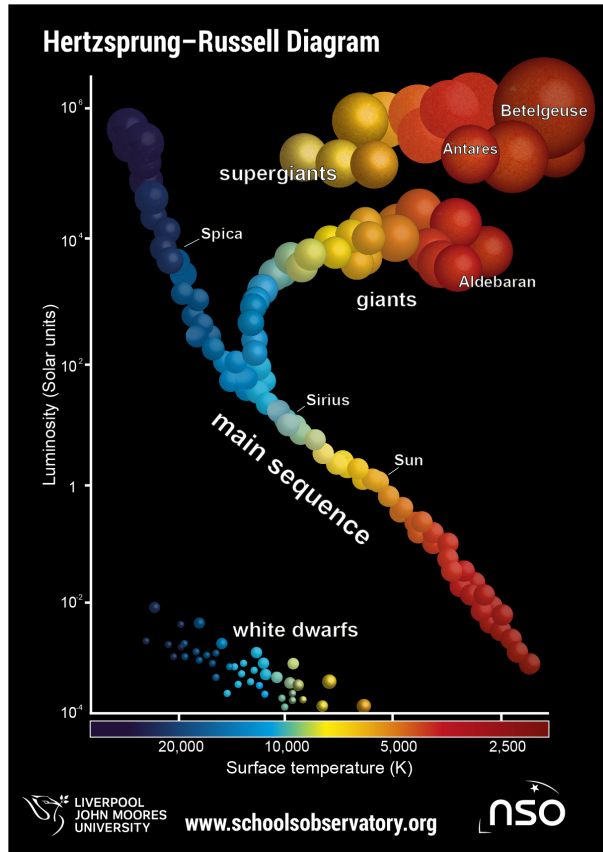
Figure 3: Example of an H-R Diagram, illustrating specific groupings that appear in the relation between temperature and luminosity of stellar bodies [4].

known as dwarf stars.

This project involved producing H-R diagrams comparing the absolute magnitude, versus the color indices of two different star clusters. Data was retrieved by taking photos of each stellar cluster with four different SDSS filters, ultraviolet (U), green/visible light (V), red (R), and near-infrared (I). Often color indices are U-B, B-V, and V-R. Limited by the filters LCO laboratories had to offer, the color indices in the results for this project were U-V and V-R, with absolute magnitude calculated with near-infrared data.

3.1 Greater Significance

Hertzsprung-Russell diagrams can provide useful visuals to describe stellar evolution. This can allow for assumptions to be made on past galactic transformations based on current stellar behaviors.

4   Data Collection

For telescopic imaging of Messier 44 and Messier 13, the same specifications were used. SDSS filters, as seen in table 1, of ultraviolet, green, red, and near-infrared were used for 10 exposures in each with an integration time of 15 seconds. Las Cumbres Observatory's SBIG STL-3603 telescopes were utilized. The field of view is 29.2 x 19.5 arcmin and the cycle time is 14 seconds [6]. The field of view is the open, observable area that can be viewed with an optical device. The cycle time is the amount of time required to complete the assigned task, in this case, taking an image. Messier 44 sits at right ascension 08:40:24.0 and declination 19:59:00. Messier 13 has right ascension 16:41:41.42 and declination 36:27:25.5. During the time of observation, the seasonal visibility, found by using LCO's Visibility Tool [9], as seen in Figures 4.1 and 4.2. The Sloan Digital Sky Survey's (SDSS) color filters were selected for their ability to let in light around specific wavelengths and for the filtering options they provide. As can be seen from Table 1, the green filter has the largest bandwidth, as it covers the peak of the visible light spectrum.

Filter	Wavelength (Angstroms)	Bandwidth (Angstroms)
Ultraviolet (u)	3543	570
Green (g)	4770	1500
Red (r)	6231	1390
Near Infrared (i)	7625	1290

Table 1: The wavelength center and wavelength width of each SDSS color filter (excluding the SDSS z filter, full infrared).

These filters are one of the most important and common photometric systems in common astronomy. Their wavelengths are visualized in Figure 4
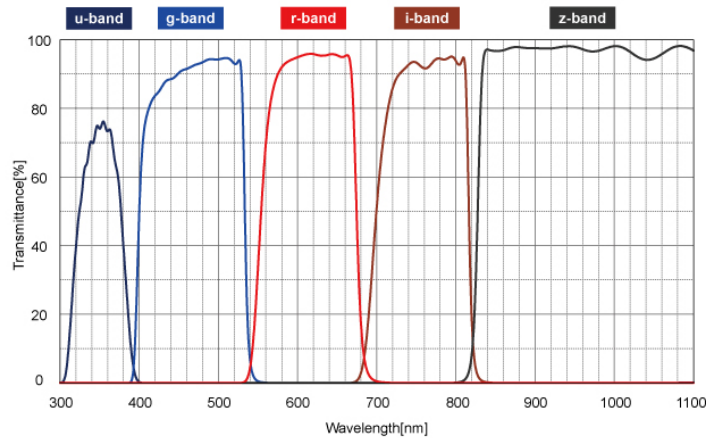

Figure 4: Graph plotting wavelength (nm) versus transmittance (%) of the SDSS filters.[7]
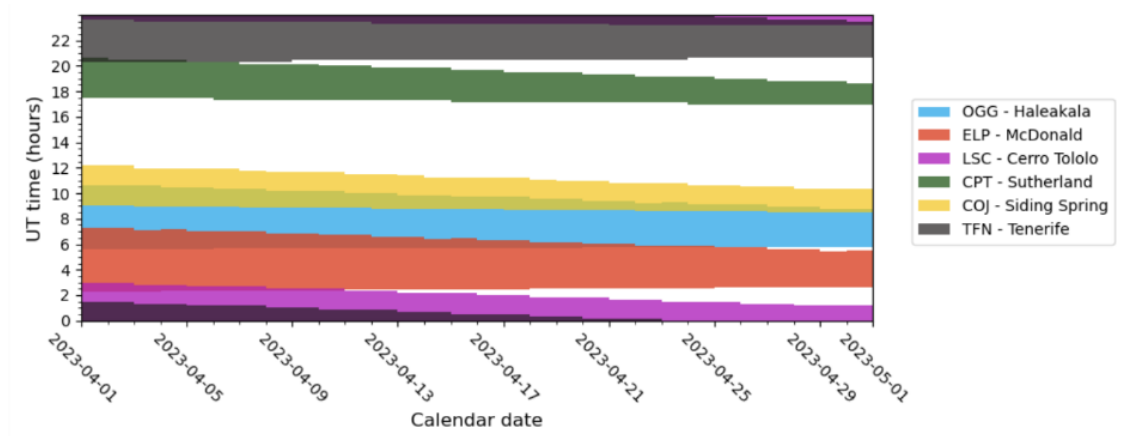
4.1 Messier 44

Figure 5: The visibility of Messier 44 rapidly decreased going into May, so images were taken in April.
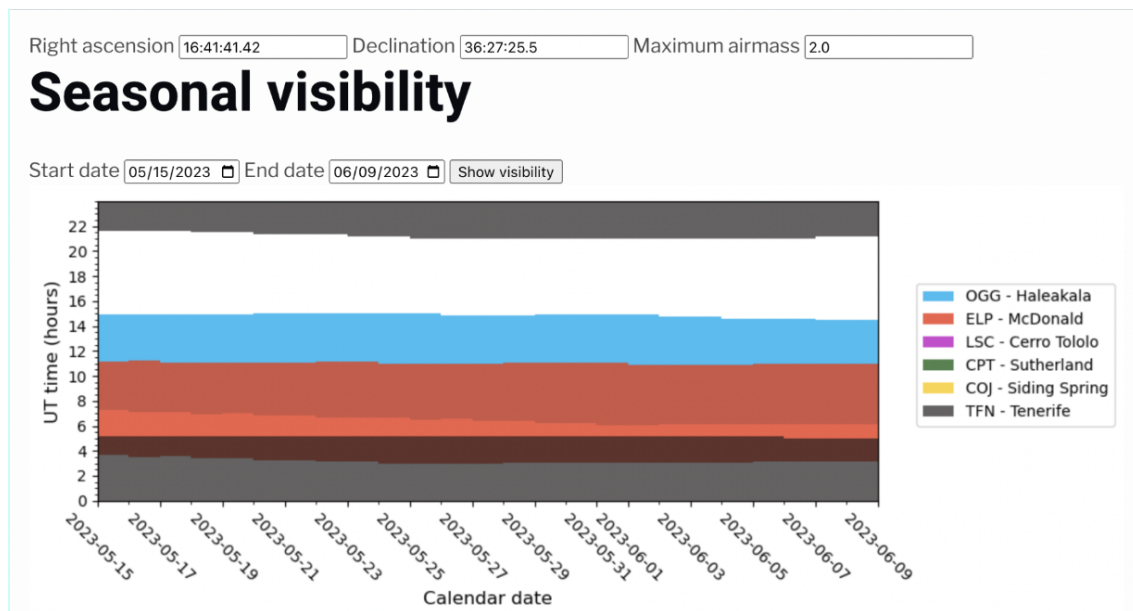
4.2 Messier 13

Figure 6: The visibility of Messier 13 was consistently strong from at least three observation sites that Las Cumbres Observatory uses.

5   Image Processing

First AstroPy was used to reformat the images sent from LCO so that they were Python-friendly. Then, stacking for composites was completed with the Python code shown below in Figures 5.1. In comparison to Figure 1 the composite image created of Messier 44, see Figure 8, lacked blue coloring and visibility of more minor stars. Similarly, the composite image of Messier 13, Figure 10, when compared to the professional image seen in Figure 2 lacks blue coloring and visibility of fringe stars on the edge of the cluster. The final image created for this project is significantly redder and less dense with small stars. This is larger due to filter selection and exposure times when taking images. The composite images could be improved if Bessel filters were used instead of SDSS, which slightly limited the usefulness of the resulting images.

5.1   Image Stacking

Figure 7: Individual images of Messier 44 from the first exposure with applied near-infrared, green, red, and ultraviolet filters.

Figure 8: The composite image of Messier 44 created by layering all 4 filtered images shown in Figure 7.
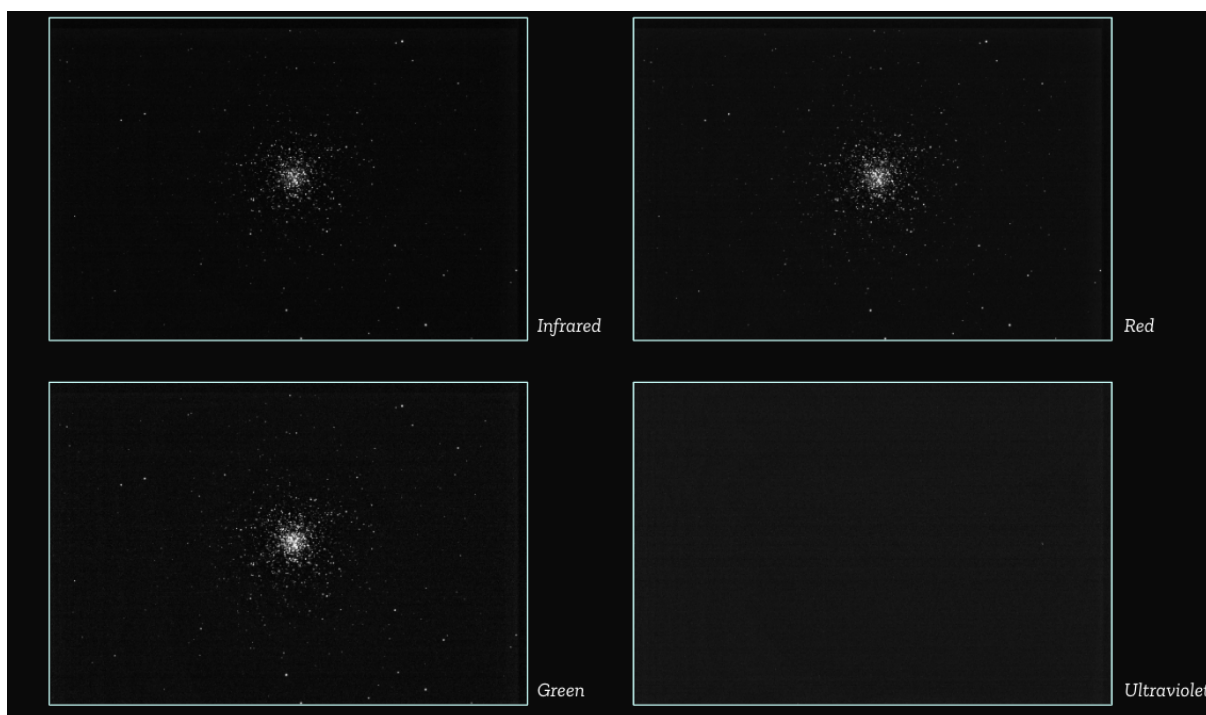

Infrared

Red

Green

Ultraviolet

Figure 9: Individual images of Messier 13 from the first exposure with near-infrared, green, red, and ultraviolet filters.

Figure 10: The composite image of Messier 13 created by layering all images in Figure 5.1

```
1 x# stacking IRGB files
2 from astropy.io import fits
3 import numpy as np
4 import matplotlib.pyplot as plt
5
6 # set file paths
7 r_file = '/content/drive/MyDrive/Copy of tfn0m410-kb24-20230515-0063-e00.fits.fz' # exp 1
8 g_file = '/content/drive/MyDrive/Copy of tfn0m410-kb24-20230515-0053-e00.fits.fz'
9 b_file = '/content/drive/MyDrive/Copy of tfn0m410-kb24-20230515-0083-e00.fits.fz'
10 i_file = '/content/drive/MyDrive/Copy of tfn0m410-kb24-20230515-0073-e00.fits.fz'
11
12 # get the data from each .fits file
13 r_data, r_header = fits.getdata(r_file, header=True)
14 g_data, g_header = fits.getdata(g_file, header=True)
15 b_data, b_header = fits.getdata(b_file, header=True)
16 i_data, i_header = fits.getdata(i_file, header=True)
17
18 # stack the data from the .fits files
19 rgbi_array = np.stack((i_data, r_data, g_data, b_data), axis=-1)
20 rgbi_array = (rgbi_array - np.min(rgbi_array)) / (np.max(rgbi_array) - np.min(rgbi_array)) * 65535.0
21 rgbi_array = rgbi_array.astype(np.uint16)
22
23 # save the composite .fit file
24 fits.writeto('irgb_stacked_16bit.fit', rgbi_array, header=r_header, overwrite=True)
25
26
27
28 # Open the FITS file
29 hdulist = fits.open('irgb_stacked_16bit.fit')
30
31 # Extract the data
32 data = hdulist[0].data
33
34 # Convert the data to a 16-bit integer array
35 data_16bit = np.array(data, dtype=np.uint16)
36
37 # Plot and save image
38 plt.imshow(data_16bit, cmap='gray', vmin=0, vmax=2*16-1)
39 plt.axis('off')
40 plt.savefig('m13_irgb_exp1.jpg', dpi=300, bbox_inches='tight')
```

Figure 11: Python code that forms a composite image by stacking the four inputted .fitz files.

5.2 H-R Plot Generation

For the purposes of this project, it was assumed that all stars are perfect blackbodies so that the Planck function could be utilized in the following expressions. The expression

$$m = -2.5log\left(\int S(\lambda)F_\lambda d\lambda + m_0\right) \tag{2}$$

generates a magnitude value for the desired color filter. For calculating the absolute magnitude as a comparison value, an ADU of 1000 was assumed. The function to find the absolute magnitude of the cluster is

$$m_{abs} = m_{infrared} - 2.5log(ADU). \tag{3}$$

Rather than selecting individual stars for H-R plot data, the composite images were further filtered with AstroArt. Then, these images were "flattened" in Python and then the log function was applied (times -2.5). As mentioned in Section 3, only ultraviolet, green, red, and near infrared-filtered images were taken. So the color indices plotted were ultraviolet-green and green-red, rather than the more commonly used ultraviolet-blue, blue-green, and then green-red.

```python
import numpy as np
import matplotlib.pyplot as plt
from astropy.io import fits

# Read the FITS files
r_data = fits.getdata('fn073_mol36_exp1_filterrp.fits.fits')
g_data = fits.getdata('fn053_mol34_exp1_filtergp.fits.fits')
u_data = fits.getdata('fn083_mol37_exp1_filterup.fits.fits')
i_data = fits.getdata('fn063_mol35_exp1_filterip.fits.fits')

# Flatten the data arrays
r_flux = -2.5*np.log10(r_data.flatten())
g_flux = -2.5*np.log10(g_data.flatten())
u_flux = -2.5*np.log10(u_data.flatten())
i_flux = -2.5*np.log10(i_data.flatten())

# Calculate the color index
U_V = u_flux - g_flux
V_R = g_flux - r_flux

# Calculate the absolute magnitude
abs_magnitude = i_flux - 2.5 * np.log10(1000)   # Assuming a distance of 1000 parsecs

# Plot the HR diagram
plt.scatter(U_V, abs_magnitude, s=1, c='black')
plt.gca().invert_yaxis()
plt.xlabel('Color Index (u-g)')
plt.ylabel('Absolute Magnitude (i)')
plt.title('HR Diagram for Exposure 1')
plt.grid(True)
plt.show()
# Plot the HR diagram
plt.scatter(V_R, abs_magnitude, s=1, c='black')
plt.gca().invert_yaxis()
plt.xlabel('Color Index (g-r)')
plt.ylabel('Absolute Magnitude (i)')
plt.title('HR Diagram for Exposure 1')
plt.grid(True)
plt.show()
```

Figure 12: Python code that creates two separate plots of the color index (U-V and V-R) vs. absolute magnitude.
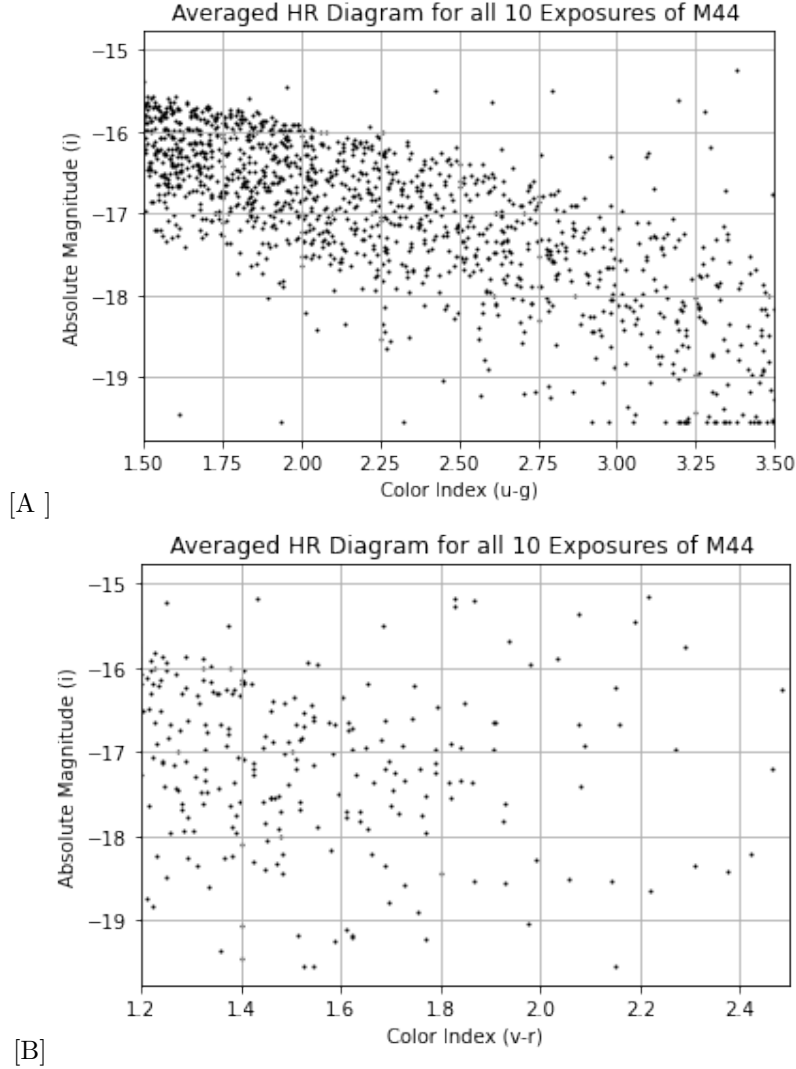
6 Analysis

[A]

[B]

Figure 13: The averaged plots for color indices u-g and v-r vs. absolute magnitude for M44 images.

As can be seen from the elements of M44 in Figure 7, the ultraviolet image filtered out the most light. When analyzing the resulting H-R plots of M44, it is clear that the red and green filtered images captured comparable data, as seen in subplot 13B, whereas the green filter retrieved far more data than the ultraviolet-filtered image which led to a higher volume of data left from taking the difference between them. There is also a clear main sequence within each subplot.

In comparison to the plots created for Messier 44, the H-R diagrams for Messier 13 have much more defined main sequences within each color index.
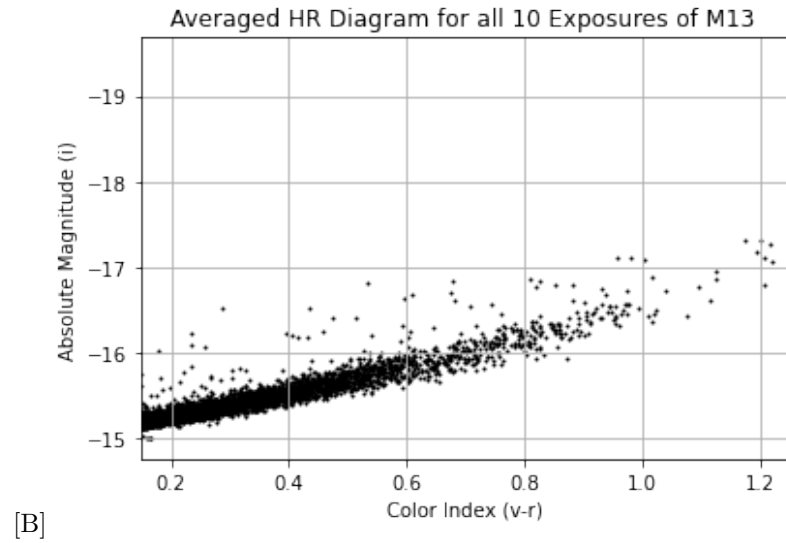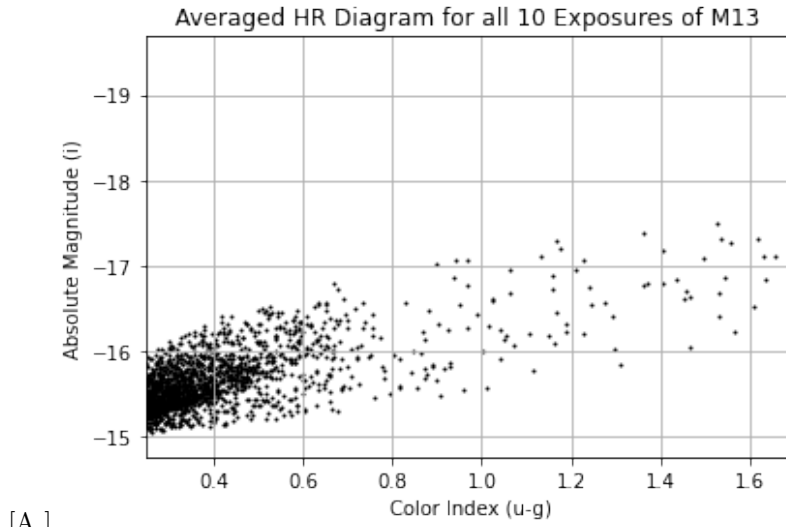
[A]

[B]

Figure 14: The averaged plots for color indices u-g and v-r vs. absolute magnitude for M13 images.

7 Error

The data collected for Messier 13 had the same observational specifications used for Messier 44. However, Messier 44 is significantly larger and closer to Earth. More stars would have likely been visible if longer exposure times were used for imaging. Additionally as mentioned in Section 5, the decision to use SDSS filters over Bessel filters limited the usability of the resulting images in H-R diagrams, specifically the lack of a blue filter. Additionally, Bessel filters are more compatible with standard magnitudes. If further work was completed on this project the following equations could have been used to convert from SDSS to Bessel magnitudes:

$$B = g + 0.3130 * (g - r) + 0.2271 \tag{4}$$

$$V = g - 0.5784 * (g - r) - 0.0038 \tag{5}$$

7.1 Signal-to-Noise Ratios

The signal (S) is the number of photons detected from a source, and the noise(N) is the total random input from varying sources. This input affects the measurement of the signal. In astronomy, a signal-to-noise ratio of about 100 can be considered an "excellent measurement" [1]. As with finding the magnitude for the Hertzrping-Russel Diagrams, a similar process was used to compute the magnitude for the signal-to-noise diagrams.

$$Mag = -2.5 * log(S) \tag{6}$$

. Where the error on the magnitude is about 1 (S/N). The values input in each array seen in Figure 17 were retrieved using AstroArt's SNR function in image processing. The values in each array for Messier 13 differed pertaining to SNR values found using AstroArt. The signal-to-noise ratio was calculated with the equation:

$$\frac{S}{N} = \frac{F A_\epsilon \sqrt{\tau}}{(\frac{N_R^2}{\tau} + F A_\epsilon + i_{DC} + F_\beta A_\epsilon \Omega)^{\frac{1}{2}}}$$

where F is flux, A_ϵ is the telescope effective area, τ is integration time, N_R is readout noise and Ω is pixel size. To convert from magnitude to flux, the following equation was used:

$$\frac{b_1}{b_2} = 10^{0.4(m_2 - m_1)}$$

where b_1 and b_2 are the fluxes of two stars and m_1 and m_2 are those stars magnitudes.

A clear trend for each stellar cluster was that the signal-to-noise ratio decreased as the magnitude increased. It can also be inferred from both Figures 15 and 16 that the signals were significantly stronger
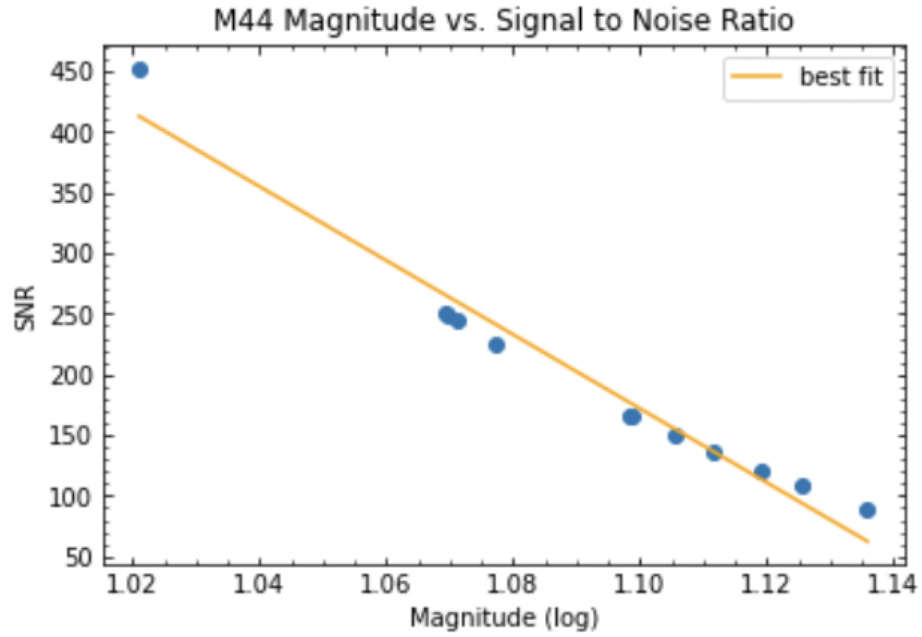
15

[-3050.71772092   3527.74545233]

Figure 15: The signal-to-noise ratio of Messier 44 stars captured plotted versus the log of the magnitude.

than the noise in both astrophotography projects. Additionally, based on the graphs, there is a good signal-to-noise ratio all the way to a magnitude of 1.14. It can be assumed from these plots that the data retrieved produced accurate measurements for analysis. According to the European Southern Observatory, the relative error for SNR is $1/SNR$. The table below displays the error for each SNR value. M44's average relative error is 0.61%, and M13's average relative error is 0.96%, as seen in the table below.
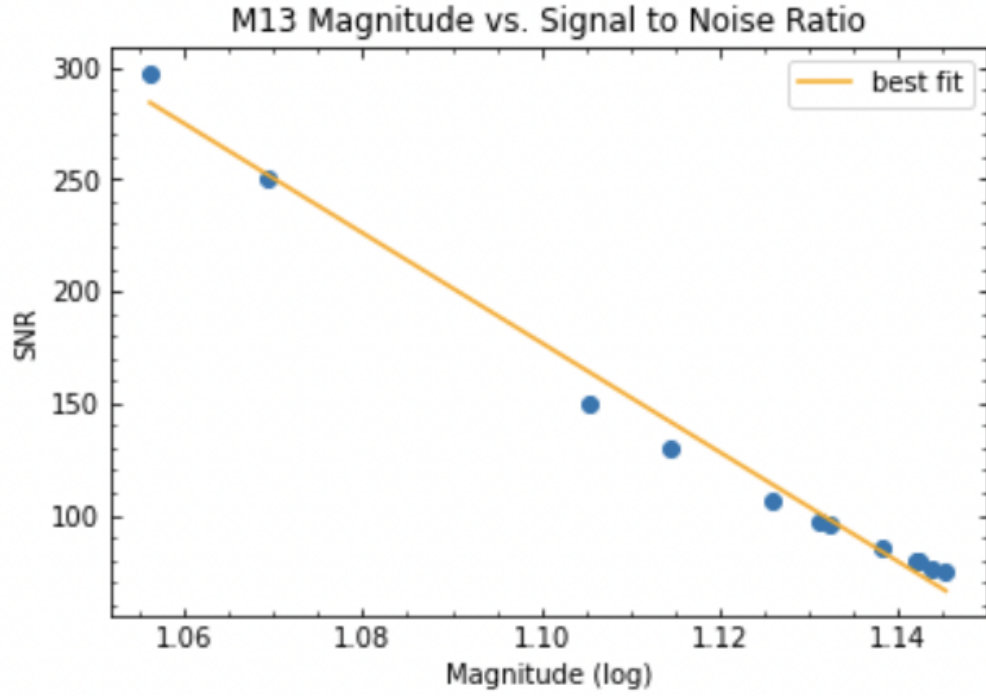
[-2438.03432809   2858.9378158]

Figure 16: The signal-to-noise ratio of Messier 13 stars captured plotted versus the log of the magnitude. A similar process was used to create this plot to the code seen in Figure 17.

SNR (M44)	Error (%) (M44)	SNR (M13)	Error (%)(M13)
452.4	0.22	297.4	0.33
250.5	0.40	250.5	0.40
249.5	0.40	150.0	0.67
244.9	0.41	129.8	0.77
225.8	0.44	107.1	0.93
166.4	0.60	97.5	1.0
166.0	0.60	95.5	1.0
149.9	0.67	85.5	1.2
135.8	0.74	79.3	1.3
120.5	0.83	79.1	1.3
108.1	0.93	76.7	1.3
89.5	1.1	74.4	1.3

17

```
from matplotlib import rc

x = np.array([10.496, 11.733, 11.741, 11.779, 11.944, 12.547, 12.552, 12.748, 12.933, 13.152, 13.346, 13.673])
y = np.array([452.5, 250.5, 249.5, 244.9, 225.8, 166.4, 166, 149.9, 135.8, 120.5, 108.1, 89.5])
# magnitude data from AstroArt
# SNR data from LCO calculator
xlog = np.log10(x)
curve = np.polyfit(xlog, y, 1)
print(curve)

rc('xtick', **{'direction' : 'in', 'top': True, 'minor.visible' : True}) # tick marks go in and adding minor tick
rc('ytick', **{'direction' : 'in', 'right': True, 'minor.visible' : True})

plt.plot(xlog, -3050.71772092*xlog + 3527.74545233, color = "orange", label = "best fit")
plt.scatter(xlog, y)
plt.legend()
plt.xlabel('Magnitude (log)')
plt.ylabel('SNR')
plt.title('M44 Magnitude vs. Signal to Noise Ratio')

plt.show()

[-3050.71772092  3527.74545233]
```

Figure 17: This Python code generates the signal-to-noise ratio plot seen in Figure 15.

8   Conclusion

The precise imaging captured for both Messier 44 and 13 provided sufficient data for the analysis of their color indices. If further work could be done on this project, the cluster ages could have been estimated with the collected data and compared to actual values. In terms of planning, it would have been useful to have implemented a longer exposure time when capturing images of Messier 13. Additionally, imaging of reference stars would have provided a more accurate absolute magnitude value for both H-R plots. Further use of AstroArt's star atlas could have also provided the project with a more accurate absolute magnitude for each star cluster. Another beneficial alteration would be transposing multiple images to reduce the background noise of the final image used for analysis. In terms of filter selection, the SDSS filters did provide a nice variety, but Bessel filters would have been better suited for the project goals. Overall, this project could have used many alterations in the initial phases of planning for the astrophotography step.

References

[1] Hainaut, O. "Signal, Noise and Detection." Signal and Noises, 1 June 2005, www.eso.org/ ohainaut/ccd/sn.html

[2] "Introduction to the Hertzsprung-Russell Diagram." Introduction to the Hertzsprung-Russell Diagram, 21 Apr. 2023, www.atnf.csiro.au/outreach/education/senior/astrophysics/stellarevolution_hrintro.

[3] "Messier 13: Hercules Globular Cluster." Messier Objects, 31 Mar. 2015, www.messier-objects.com/messier-13-hercules-globular-cluster/.

[4] "National Schools' Observatory." Hertzsprung-Russell Diagram — National Schools' Observatory, 2012, www.schoolsobservatory.org/learn/astro/stars/class/hrdiagram.

[5] "Praesepe (M44): The Beehive Cluster." Constellation Guide, 26 June 2014, www.constellation-guide.com/praesepe-m44-the-beehive-cluster/.

[6] "SBIG STL-6303." Las Cumbres Observatory, 2017, lco.global/observatory/instruments/sbig-stl-6303/.

[7] "SDSS Filters (Conventional): Asahi Spectra USA Inc.." SDSS Filters (Conventional) — Asahi Spectra USA Inc., www.asahi-spectra.com/opticalfilters/sdss.asp. Accessed 6 June 2023.

[8] "SDSS Filters." Sky Server, 2012, skyserver.sdss.org/dr1/en/proj/advanced/color/sdssfilters.asp.

[9] "Visibility Tool." — Las Cumbres Observatory, lco.global/observatory/tools/visibility/. Accessed 25 May 2023.